Mechanics of Advanced Composite Structures

Journal homepage: https://macs.semnan.ac.ir/

Semnan University

ISSN: 2423-7043

Research Article

Homogenisation-Based Analytical–Numerical Modelling of Orthogonal Trapezoidal Corrugated-Core Sandwich Panels

Sanaz Sanjarian [a], Pooria Akbarzadeh [b*]

[a] *Master's Graduate in Mechanical Engineering, University of Sistan and Baluchestan, Zahedan, Iran*

[b] *Assistant Professor, Department of Mechanical Engineering, University of Sistan and Baluchestan, Zahedan, Iran*

ARTICLE INFO

Article history:

Received: 2025-12-8

Revised: 2025-**-**

Accepted: 2025-**-**

Keywords:

Sandwich panels;
trapezoidal corrugated core;
homogenisation;
finite element analysis;
Geometry-induced orthotropy;

ABSTRACT

This study investigates the mechanical behaviour of sandwich panels incorporating orthogonal trapezoidal corrugated cores subjected to uniformly distributed transverse loading. Owing to the inherently three-dimensional folded architecture of such cores, accurately predicting their global response poses significant modelling challenges. To address this complexity, a homogenisation-based analytical framework is developed by integrating Classical Plate Theory (CPT) with an equivalent orthotropic representation in which the stiffness arises purely from geometry-induced anisotropy. The analytical predictions are rigorously validated through detailed finite element simulations in ABAQUS using an isotropic aluminium material model, ensuring consistency between the homogenised assumptions and the numerical reference.

A comprehensive parametric study is performed to quantify the influence of key geometric descriptors—including wave height, crown width, half-wave length, core thickness, and face-sheet thickness—on global deflection and von Mises stress distribution. The results demonstrate that increasing wave height from 10 to 30 mm reduces maximum deflection by approximately 18%, while a 2-mm increase in face-sheet thickness lowers peak stress by nearly 12%. The analytical and numerical responses exhibit excellent agreement, with an average deviation of about 2% within the validated range, thereby establishing a clear and practically useful validity range for the proposed homogenisation approach.

Overall, the findings provide quantitative insight into how orthogonal corrugation geometry governs equivalent stiffness, deformation patterns, and stress behaviour. The developed framework offers a validated, computationally efficient alternative to full 3D modelling and can serve as a practical tool for the preliminary design and optimisation of lightweight corrugated-core sandwich structures used in aerospace, marine, and automotive applications.

1. Introduction

Sandwich panels are widely employed in aerospace, marine, and automotive structures owing to their high bending stiffness and strength at low weight. Among various core topologies, trapezoidal corrugated profiles are particularly attractive due to their efficient load-carrying capability and ability to redistribute stresses through geometry-induced stiffness. In such systems, global deformation and stress response are strongly governed by geometric descriptors including wave height, crown width, and face-sheet thickness, making systematic geometric evaluation essential for informed design.

* **Corresponding author.**
E-mail address: *p.akbarzadeh@eng.usb.ac.ir,*

Cite this article as:

Sanjarian, S. and Akbarzadeh, P., 2026. Homogenisation-Based. *Mechanics of Advanced Composite Structures*, 13(1), pp. xxx-xxx.
https://doi.org/10.22075/MACS.2025.39315.2050

However, the inherently folded three-dimensional architecture of corrugated cores limits the direct use of classical plate formulations. This three-dimensional folded layout leads to locally varying curvature and alternating inclined segments, violating the fundamental assumption of Classical Plate Theory that plane sections remain plane and normal to the mid-surface after deformation. As a result, direct use of CPT on the corrugated geometry would neglect local bending–shear coupling and inter-fold curvature effects, thereby motivating an equivalent homogenised representation at the unit-cell level. Homogenisation techniques have therefore been adopted to replace the corrugated geometry with an equivalent orthotropic plate whose stiffness arises purely from geometry. Although this approach has been successful for several corrugation types, orthogonal trapezoidal configurations—where corrugations are arranged along two perpendicular directions—remain insufficiently explored. Their multi-directional stiffness interactions differ fundamentally from single-direction cores, revealing a clear gap in analytical modelling capabilities.

The present study addresses this gap by analysing sandwich panels equipped with three orthogonal trapezoidal corrugated cores and four aluminium face sheets under uniformly distributed transverse loading. A combined analytical–numerical framework is developed: (i) an extended homogenisation procedure integrated with Classical Plate Theory (CPT) to establish the equivalent orthotropic stiffness, and (ii) finite element simulations in ABAQUS using an isotropic aluminium material model for validation. Key geometric parameters—wave height, crown width, half-wave length, core thickness, and face-sheet thickness—are systematically varied to quantify their influence on deflection and von Mises stress. The study aims to (1) formulate an analytical model tailored to orthogonal trapezoidal cores, (2) determine the validity range of the homogenisation method, and (3) provide design-oriented geometric guidelines.

By quantifying how geometry governs stiffness and stress response, and by demonstrating strong agreement between analytical predictions and full 3D simulations, the proposed framework offers a reliable and computationally efficient tool for early-stage design of corrugated-core sandwich structures. From an application perspective, the proposed homogenisation-based framework is particularly suited for preliminary design and optimisation stages, where rapid evaluation of geometric configurations is required without resorting to full three-dimensional finite element modelling. The ability to quantify the influence of key geometric parameters and to establish a validated applicability range makes the approach relevant for lightweight structural components in aerospace panels, marine decks, and automotive sandwich structures, where stiffness-to-weight efficiency and computational efficiency are critical design considerations.

The remainder of the paper is organised as follows: Section 2 reviews analytical and homogenisation studies; Section 3 introduces the material system, geometry, and methodology; Section 4 presents and discusses the parametric results; and Section 5 summarises the main findings.

2. Literature Review

The development of composite and corrugated core sandwich panels has attracted growing research interest due to the increasing demand for lightweight, high-stiffness, and high-efficiency structural components. Early studies, such as Sutherland et al. [1], provided foundational understanding of the dynamic and quasi-static behaviour of glass fiber reinforced sandwich structures, establishing baseline insights into impact resistance and fatigue performance. Reinforcement techniques—including the resin-pin approach introduced by Ivazian et al. [2]—further highlighted strategies for enhancing stiffness, indentation strength, and long-term durability.

Significant progress in corrugated core design was achieved through the works of Li et al. [3] and Abada and Ibrahim [4], who demonstrated the strong influence of geometric attributes such as crown width, corrugation angle, and face sheet thickness on load transfer, shear stability, and blast resistance, as also reported in several related studies addressing geometry-induced stress distribution and structural performance of folded cores [5,6]. Complementary experimental–numerical research by Jin et al. [7] on auxetic honeycomb systems and Mahdiabadi et al. [8] on energy-absorbing corrugated profiles expanded understanding of deformation mechanisms under dynamic loads. Parametric investigations reported by Long et al. [9] and Xia et al. [10] provided further clarification of how geometric and material parameters govern global stiffness and local failure modes.

On the analytical modeling front, higher-order plate formulations proposed by Matsunaga [11] and refined analytical solutions from Zhen and Ren [12] improved the prediction of transverse deformation and localized effects in sandwich plates. Homogenization techniques have also contributed substantially to analytical modeling; for instance, Huang et al. [13] established reliable

equivalent-medium representations for orthogonal lattice metamaterials.

Building on these foundations, Hashemi et al. [14] developed a homogenization-based analytical framework for cross-arranged trapezoidal and sinusoidal corrugated cores (three-layer cores with four isotropic aluminum face sheets), incorporating classical plate theory and validating the model using ABAQUS. Their comparisons showed strong agreement with benchmark results (errors <4.3% relative to Xia et al. [10]).

To clearly distinguish the present study from Hashemi's work, the primary methodological differences are summarized in Table 1.

Extending the homogenization methodology, the present work introduces three major advancements:
(1) a systematic five-parameter geometric sensitivity analysis,
(2) formulation of a quantitative validity range to support preliminary engineering design, and (3) application of statistical performance metrics (RMSE and R^2) to assess model reliability across a wide set of practical geometries.

Recent developments, such as multiscale and hybrid modeling frameworks by Kamareh et al. [15] and emerging machine-learning-driven optimization strategies highlighted by Wang et al. [16], further underscore the rapid evolution of design tools for corrugated and architected sandwich structures.

Despite these advances, the combined homogenization-based analytical modeling and full finite element validation of orthogonal trapezoidal corrugated cores—along with a comprehensive geometric sensitivity evaluation—remains insufficiently explored. The present study directly addresses this gap by establishing an analytical framework tailored to this specific core architecture and by rigorously validating its predictive capability over an extensive design space.

3. Materials and Methods

3.1. Geometric Configuration and Material Properties

The sandwich panel examined in this study consists of four flat face sheets and three orthogonal trapezoidal corrugated cores arranged in a cross-pattern, as illustrated in Figure 1.

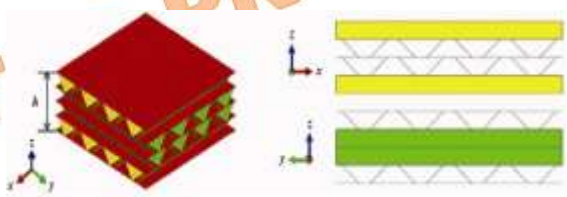

Fig. 1. Schematic of sandwich panel with orthogonal trapezoidal corrugated core

The panel is subjected to a uniformly distributed transverse load and is simply supported along all its edges. Key geometric parameters include the wave height (h), crown width (w), half-wave length (c), core thickness (t_c), and face-sheet thickness (t_f). These geometric descriptors are systematically varied to quantify their influence on global bending response and stress distribution. Detailed geometric definitions are provided in Figure 2.

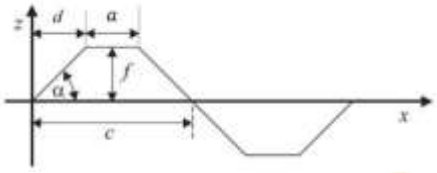

Fig. 2. Detailed geometric specifications of the trapezoidal corrugated core, illustrating the definition of the geometric parameters and the investigated dimensional ranges (a = 20–40 mm, d = 3–8 mm, f = 10–30 mm, c = 15–35 mm).

Table 1. Key Distinctions Between Hashemi et al. (2020) and the Present Study

Feature	Hashemi et al. (2020)	Present Study
Core Geometry	Trapezoidal + sinusoidal (cross-arranged)	Orthogonal trapezoidal corrugation
Materials	Isotropic aluminum	Isotropic aluminum (geometry-induced orthotropy)
Parametric Study	Limited (e.g., thickness, amplitude)	Five-parameter analysis (h, w, c, t_c, t_f)
Validation Approach	Analytical–FEM (<4.3% error)	Statistical validation (RMSE, ~2% avg. error within the validated range)
Design Contribution	Performance comparison	Quantitative validity range (t/l = 0.06–0.08)

Both the face sheets and the corrugated cores are modelled as isotropic aluminium with identical elastic properties. Although the actual material is isotropic, the effective orthotropic behaviour observed at the panel level arises purely from the geometry-induced anisotropy of the trapezoidal corrugation. The elastic modulus, Poisson's ratio, and density used in both the analytical and numerical models are summarised in Table 2.

Table 2. Material Properties of Sandwich Panel Components

Component	Elastic Modulus (GPa)	Poisson's Ratio	Density (kg/m^3)
Face Sheet	70	0.33	2700
Corrugated Core	70	0.33	2700

3.2. Analytical Framework: Homogenization and Classical Plate Theory

The analytical model combines homogenisation techniques with Classical Plate Theory (CPT) to predict the structural response of the sandwich panel. The complex three-dimensional geometry of the orthogonal trapezoidal corrugated core is replaced by an equivalent orthotropic flat plate, as illustrated in Figure 3. This equivalent representation significantly reduces computational cost while preserving the essential bending and membrane stiffness characteristics induced by the corrugation geometry.

Fig. 3. Homogenization of corrugated sheet to equivalent orthotropic plate

3.2.1 Homogenization of the Trapezoidal Corrugated Core

Homogenisation is performed based on the strain-energy equivalence principle, which requires the strain energy of a representative unit cell of the corrugated core to match that of an equivalent flat orthotropic plate subjected to identical deformation modes, following established homogenisation formulations for corrugated structures (Briassoulis [17]; Hashemi et al. [14]).

A representative unit cell corresponds to one half-period of the corrugation, defined by the half-wave length (c), wave height (h), crown width (w), and sheet thickness (t_c). The inclined segment length is given in Eq. (1):

$$l = \sqrt{h^2 + \left(\frac{c-w}{2}\right)^2} \tag{1}$$

The developed length of the corrugation within one half-period is $L = w + 2l$. The mid-surface position vector is described as expressed in Eq. (2):

$$\vec{R}(x) = x\hat{\imath} + f(x)\hat{k} \tag{2}$$

where $f(x)$ denotes the piecewise function representing the trapezoidal shape. Similar geometric descriptions and strain-energy-based homogenization procedures for trapezoidal corrugated unit cells can be found in Refs. [14,17]. The homogenization procedure yields the effective extensional and bending rigidities of the equivalent orthotropic plate. The generalized constitutive relation linking in-plane forces (N_x, N_y, N_{xy}) and bending moments (M_x, M_y, M_{xy}) to membrane strains (ε^0_x, ε^0_y, γ^0_{xy}) and curvatures (κ_x, κ_y, κ_{xy}) is given in Eq. (3):

$$\begin{bmatrix} N_x \\ N_y \\ N_{xy} \\ M_x \\ M_y \\ M_{xy} \end{bmatrix} = \begin{bmatrix} A_{11} & A_{12} & 0 & 0 & 0 & 0 \\ A_{21} & A_{22} & 0 & 0 & 0 & 0 \\ 0 & 0 & A_{66} & 0 & 0 & 0 \\ 0 & 0 & 0 & D_{11} & D_{12} & 0 \\ 0 & 0 & 0 & D_{21} & D_{22} & 0 \\ 0 & 0 & 0 & 0 & 0 & D_{66} \end{bmatrix} \begin{bmatrix} \varepsilon^0_x \\ \varepsilon^0_y \\ \varepsilon^0_{xy} \\ \kappa_x \\ \kappa_y \\ \kappa_{xy} \end{bmatrix} \tag{3}$$

where [A], [B], and [D] are the 3×3 matrices representing the extensional, coupling, and bending stiffnesses, respectively. Due to the geometric symmetry of the core about its mid-plane, the coupling matrix [B] is zero (B_{ij}= 0), decoupling the in-plane and bending responses, consistent with classical laminated plate formulations (Reddy [18]; Matsunaga [11]).

The non-zero stiffness terms for the equivalent orthotropic plate are derived based on the unit cell geometry and material properties (Young's modulus E and Poisson's ratio ν) of the core material. The key stiffness coefficients are presented in Table 3.

The stiffnesses are computed by applying six fundamental deformation modes—uniaxial stretching (x, y), pure shear, bending about x and y axes, and torsion—to the unit cell. The resulting forces and moments populate the equivalent stiffness matrix D. Table 4 summarizes the applied boundary conditions.

3.2.2 Governing Equations for the Sandwich Panel

After obtaining the equivalent orthotropic properties of the corrugated core through homogenisation, the face sheets and the core are assembled into a multi-layered laminate.

According to Classical Plate Theory (CPT), the displacement field *(u, v, w)* at any point *(x, y, z)* is expressed as shown in Eq. (4):

$$u(x,y,z) = u_0(x,y) - z\frac{\partial w_0}{\partial x}$$
$$v(x,y,z) = v_0(x,y) - z\frac{\partial w_0}{\partial y} \quad (4)$$
$$w(x,y,z) = w_0(x,y)$$

where the mid-surface displacements fully determine the deformation of the plate, and the transverse normals are assumed to remain straight and perpendicular to the mid-surface throughout bending. This assumption is consistent with small-strain, moderately thick plate behaviour and is widely adopted for sandwich panels with relatively stiff face sheets (Matsunaga [11]; Reddy [18]).

Table 3. Equivalent Stiffness Expressions for the Trapezoidal Corrugated Core

D_{11}	$\frac{E\,t_c^3}{12(1-\nu^2)}\frac{L}{c}$	Bending stiffness in the corrugation direction
D_{22}	$\frac{E\,c\,I_y}{L}$	Bending stiffness transverse to corrugations
D_{12}	νD_{22}	Coupling bending stiffness
D_{66}	$\frac{E\,c\,t_c^3}{12L} + \frac{E\,h^2 t_c (c-w)^2}{2cL}$	Torsional stiffness
A_{11}	$\frac{E\,t_c\,L}{c}$	Extensional stiffness in the corrugation direction
A_{22}	$\frac{E\,t_c\,c}{L}$	Extensional stiffness transverse to corrugations
A_{12}	0	In-plane shear coupling
A_{66}	$G\,t_c\frac{c}{L}$ *where* $G = \frac{E}{2(1+\nu)}$	In-plane shear stiffness

Table 4. Boundary Conditions Applied to the Unit Cell for Stiffness Calculation

1	Uniaxial tension *(x)*	$\varepsilon_x^0 = 1, all\ other\ strains/curvatures = 0$
2	Uniaxial tension *(y)*	$\varepsilon_y^0 = 1, all\ other\ strains/curvatures = 0$
3	Pure bending *(x)*	$\kappa_x = 1, all\ other\ strains/curvatures = 0$
4	Pure bending *(y)*	$\kappa_y = 1, all\ other\ strains/curvatures = 0$
5	Pure in-plane shear	$\gamma_{xy}^0 = 1, all\ other\ strains/curvatures = 0$
6	Pure torsion	$\kappa_{xy} = 1, all\ other\ strains/curvatures = 0$

The overall extensional, coupling, and bending stiffness matrices [A], [B], and [D] are computed by integrating the contributions of all layers using the parallel-axis theorem, as expressed in Eq. (5):

$$[A]=\sum_{k=1}^{N}\left[\bar{Q}\right]_k (z_k - z_{k-1})$$
$$[B]=\frac{1}{2}\sum_{k=1}^{N}\left[\bar{Q}\right]_k (z_k^2 - z_{k-1}^2) \quad (5)$$
$$[D]=\frac{1}{3}\sum_{k=1}^{N}\left[\bar{Q}\right]_k (z_k^3 - z_{k-1}^3)$$

where $\left[\bar{Q}\right]_k$ is the transformed reduced stiffness matrix of the *k*-th layer, and z_k represents its distance from the global mid-plane. For the face sheets, the stiffness matrix $[Q]$ corresponds to isotropic material behaviour, while for the core, the orthotropic matrix derived from homogenization is used.

For the orthogonal corrugated configuration considered in this study, each trapezoidal corrugated sheet is first homogenised independently. The resulting equivalent orthotropic stiffness matrices are then assembled at the equivalent plate level using Classical Plate Theory. To account for the orthogonal arrangement of the corrugated cores, the stiffness matrix of the orthogonally oriented corrugated layer is rotated into the global coordinate system prior to integration using standard stiffness transformation relations. The global [A], [B], and [D] matrices therefore represent the combined contribution of the homogenised corrugated layers and face sheets through thickness integration, rather than a direct superposition of individual core stiffnesses. The governing differential equation for an orthotropic plate subjected to a uniformly distributed load *q* is given by Eq. (6):

$$D_{11}\frac{\partial^4 w_0}{\partial x^4} + 2(D_{12}+2D_{66})\frac{\partial^4 w_0}{\partial x^2 \partial y^2} + D_{22}\frac{\partial^4 w_0}{\partial y^4} = q \quad (6)$$

For a simply supported rectangular plate of dimensions $a \times b$, the boundary conditions are defined by Eqs. (7) and (8):

$$\text{At } x=0,a: \; w_0 = 0,$$
$$M_x = -D_{11}\frac{\partial^2 w_0}{\partial x^2} - D_{12}\frac{\partial^2 w_0}{\partial y^2} = 0 \quad (7)$$

$$\text{At } y=0,b: \; w_0 = 0,$$
$$M_y = -D_{12}\frac{\partial^2 w_0}{\partial x^2} - D_{22}\frac{\partial^2 w_0}{\partial y^2} = 0 \quad (8)$$

The deflection field *w(x, y)* is obtained using the Navier series solution, which inherently satisfies the boundary conditions, as given in Eq. (9):

$$w_0(x,y)=\sum_{m=1}^{\infty}\sum_{n=1}^{\infty} W_{mn}\sin\left(\frac{m\pi x}{a}\right)\sin\left(\frac{n\pi y}{b}\right) \quad (9)$$

Solving the resulting system yields coefficients W_{mn}, from which deflection and stress distributions are derived, following classical Navier-type solutions for orthotropic and sandwich plates (Matsunaga [11]; Reddy [18]).

Although the von Mises stress is not introduced as a separate governing equation, it is directly derived from the in-plane normal and shear stresses obtained within the Classical Plate Theory framework. The membrane strains and curvatures calculated from the force and bending-moment resultants are first used to evaluate the stress components at the top and bottom face sheets. The von Mises stress is then computed under plane-stress conditions using the standard von Mises criterion.

3.3. Numerical Simulation in ABAQUS

Finite element simulations are carried out in ABAQUS/Standard 2022 (Dassault Systèmes, France) to validate the analytical predictions obtained from the homogenised equivalent-plate model. The full three-dimensional geometry of the sandwich panel, including the flat face sheets and the orthogonal trapezoidal corrugated cores, is modelled to provide a high-fidelity reference solution. The face sheets and cores are assigned isotropic aluminium properties consistent with Table 2, and surface-to-surface tie constraints are used to represent adhesive bonding between components (Figure 4).

The tie constraint enforces a perfectly bonded face–core interface, consistent with the Classical Plate Theory assumptions of the analytical model. While localised stress concentrations may occur at sharp geometric transitions, such effects are confined to small regions and do not affect the global response measures (deflection and representative von Mises stress) used for validation.

A mesh-convergence study is performed to ensure numerical accuracy, with local refinement applied near regions susceptible to high stress gradients, particularly along corrugation folds and face–core interfaces (Figure 5). The converged finite element discretisation consists

of approximately 100,000–150,000 quadrilateral shell elements (S4R), corresponding to about 110,000–160,000 nodes depending on the face-sheet thickness and corrugation geometry. This mesh density is consistent with previous finite element studies on cross-arranged corrugated-core sandwich panels [14], and was selected based on convergence of global response quantities, namely maximum transverse deflection and representative von Mises stress. A uniformly distributed transverse pressure is applied to the top surface, and simply supported boundary conditions are enforced along all four edges.

Deflection contours and von Mises stress distributions extracted from the 3D ABAQUS model are compared with results from the homogenised analytical formulation. Model verification is carried out by quantitatively evaluating the agreement between analytical and numerical results using global response quantities, with statistical performance metrics including the root mean square error (RMSE) and the coefficient of determination (R^2) employed to assess accuracy across the investigated configurations. This comparison provides a quantitative assessment of the accuracy and applicability limits of the homogenisation-based equivalent-plate model.

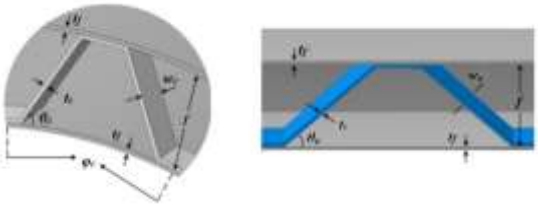

Fig. 4. Adhesive connection between flat sheet and trapezoidal corrugated core

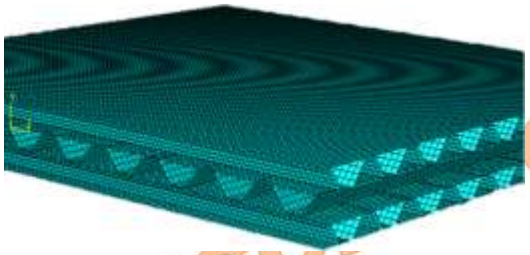

Fig. 5. Meshed geometry of the sandwich panel

3.4. Parametric Study Design

A comprehensive parametric study is conducted to evaluate the influence of key geometric descriptors on the global bending response of the sandwich panel. The parameters investigated include wave height (10–30 mm), crown width, half-wave length, core thickness, and face-sheet thickness, varied within practical engineering ranges. For each configuration, both the maximum deflection and peak von Mises stress are recorded from analytical and numerical models.

The resulting trends are used to identify geometric combinations that yield enhanced stiffness and reduced stress concentration. By quantifying the sensitivity of global response to geometry, this systematic exploration provides practical guidelines for the design and optimisation of orthogonal trapezoidal corrugated sandwich panels subjected to transverse loading.

4. Results and Discussion

4.1. Validation of Homogenization Method

The analytical model developed through homogenisation and Classical Plate Theory (CPT) was validated against detailed finite element simulations in ABAQUS. Table 5 presents the statistical comparison for maximum deflection, while Table 6 summarises the corresponding validation results for von Mises stress, using the analytical solution as the reference baseline. The results demonstrate strong agreement across the investigated configurations, characterised by low average errors, small RMSE values, and high coefficients of determination ($R^2 > 0.95$). In particular, within the validated face-sheet thickness range ($t_f \geq 6$ mm), the deviation reduces to approximately 2%, indicating improved accuracy of the homogenised CPT formulation as the structural response becomes bending-dominated. Figure 6 presents the deflection profiles obtained from both approaches, demonstrating near-identical trends and maximum displacement locations.

Table 5. statistical validation for maximum deflection

t(mm)	Analytical deflection (mm)	FE deflection (mm)	Error (%)
10	0.130	0.152	17.46
8	0.169	0.180	6.31
6	0.228	0.231	1.30
5	0.296	0.276	7.25
4	0.370	0.340	8.1
RMSE			0.02 mm
R^2			0.951

Table 6: Statistical validation for von Mises stress

t(mm)	Analytical σ_{mises} (MPa)	Numerical σ_{mises} (MPa)	Error (%)
6	13.13	12.30	6.3
7	11.50	10.70	7.0

8	8.80	8.50	3.4
RMSE			0.66 MPa
R^2			0.99

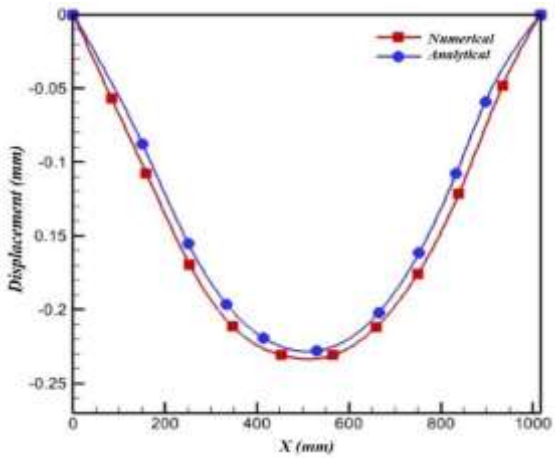

Fig. 6. Comparison of deflection profiles from analytical (CPT) and numerical methods for a reference sandwich panel configuration. The X-axis represents the distance from the plate edge.

To establish the applicability limits of the homogenisation approach, additional analyses were performed for extreme geometric variations. At significantly increased wave heights (greater than 40 mm), the numerical model exhibited localised deformation patterns and early-stage buckling modes that are not represented in CPT-based homogenisation. As a result, the analytical solution underestimated deflection by 5–7% in these cases. This deviation highlights the importance of recognising when geometry-induced local effects dominate, as such mechanisms fall outside the assumptions of classical homogenisation.

Table 7 summarises representative pointwise comparisons between the analytical and numerical results, while the overall statistical reliability of the homogenisation model across the investigated parameter space is quantitatively assessed using RMSE and R^2 metrics reported in Tables 5 and 6. The data confirm the robustness of the analytical model within typical engineering design ranges, while also defining practical limits for its use in predicting global responses. Hence, the validated homogenisation method can serve as an efficient alternative to full three-dimensional finite element models for preliminary design and parametric exploration, provided that geometric extremes are avoided.

Table 7. Comparison of Deflection and Error Percentage between Analytical and Numerical Methods

Configuration	Analytical Deflection (mm)	Numerical Deflection (mm)	Error (%)
Reference Geometry	5.23	5.34	2.06
High Wave Height	4.85	5.20	6.73

4.2. *Influence of Geometric Parameters on Deflection*

The parametric investigation demonstrates that the geometric configuration of the corrugated core plays a decisive role in governing the global deflection of the sandwich panel. Among the evaluated parameters, wave height, crown width, half-wave length, core thickness, and face-sheet thickness all exhibited measurable effects on the bending stiffness of the panel. The parametric trends discussed in this section are interpreted within the validated accuracy range of the homogenisation-based CPT model established in Section 4.1.

Increasing the wave height from 10 to 30 mm resulted in an 18% reduction in maximum deflection, primarily due to the increased second moment of area contributed by the taller corrugation webs. This reduction trend, illustrated in Figure 7 for different height ratios (f/a), is further confirmed by the numerical results shown in Figure 8.

The influence of crown width and half-wave length is summarised in Table 8. Increasing crown width to 20 mm decreased deflection by approximately 8%, while reducing the half-wave length to 15 mm increased the number of corrugation cells per unit span, enhancing stiffness by nearly 10%. These findings, illustrated in Figure 9, highlight how geometric compaction improves load distribution and raises bending rigidity.

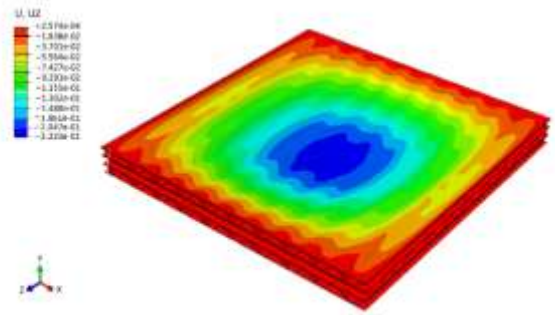

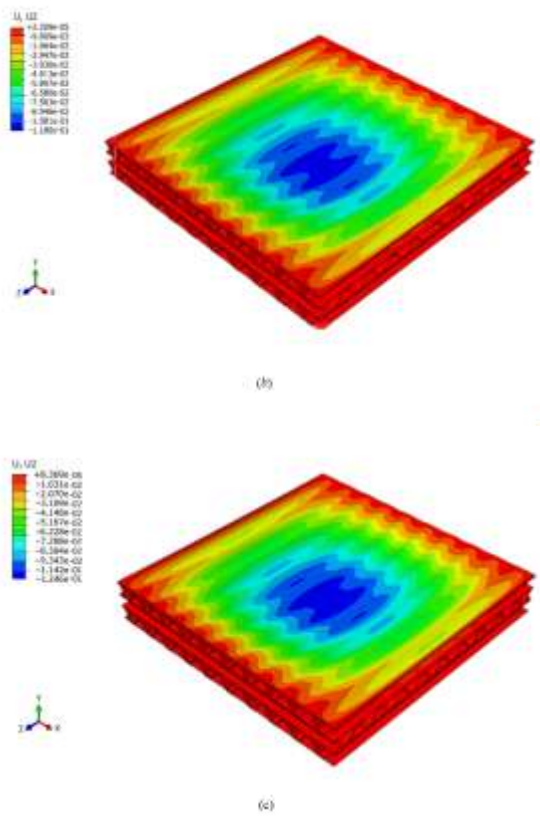

Fig. 7. Contour of deflection for varying wave height ratios (a) f/a=0.5, (b) f/a=0.7, (c) f/a=0.9

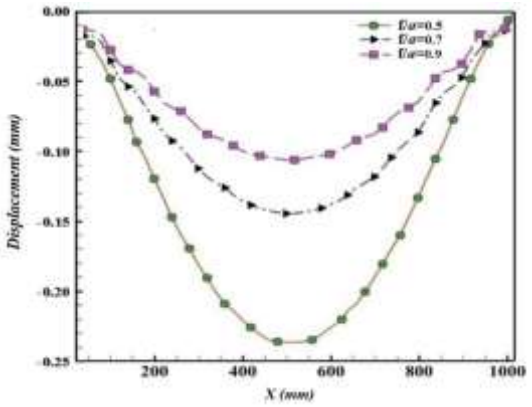

Fig. 8. Comparison of deflection for varying wave height ratios

Table 8. Deflection Variation with Crown Width and Wave Height

Parameter	Value Range	Deflection Change (%)
Crown Width (mm)	10 to 20	-8
Wave Height (mm)	10 to 30	-18

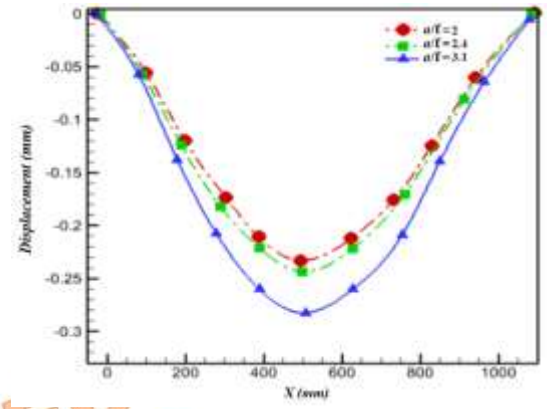

Fig. 9. Comparison of deflection for varying crown width

In addition to core geometry, thickness variations in both the corrugated core and face sheets contributed to changes in global stiffness. Increasing the core thickness by 50% produced a moderate 5% decrease in deflection, reflecting the secondary contribution of shear stiffness to the overall response. In contrast, the face-sheet thickness proved to be a dominant parameter: increasing it by 2 mm reduced deflection by approximately 12%, as shown in Figures 10 and 11.

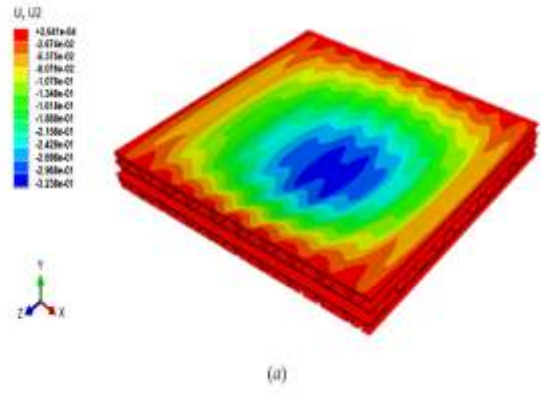

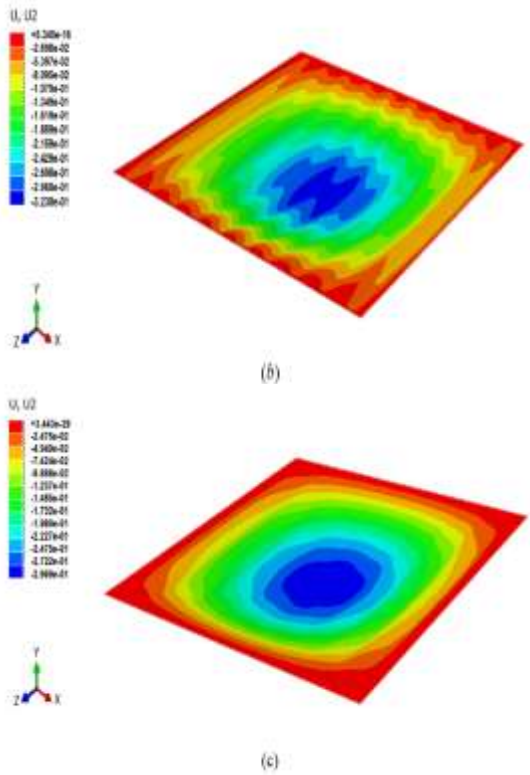

Fig. 10. Contour of deflection for face sheet thickness t=4 mm (a) sandwich panel, (b) top plate, (c) bottom plate

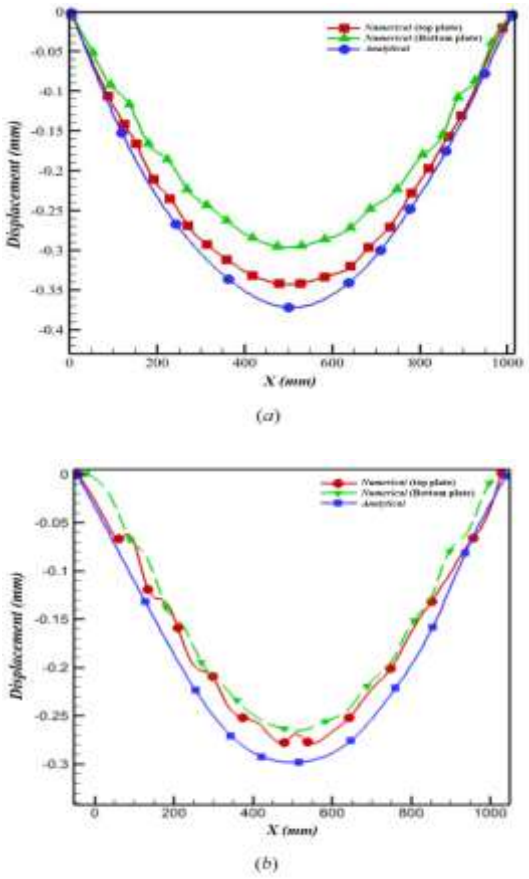

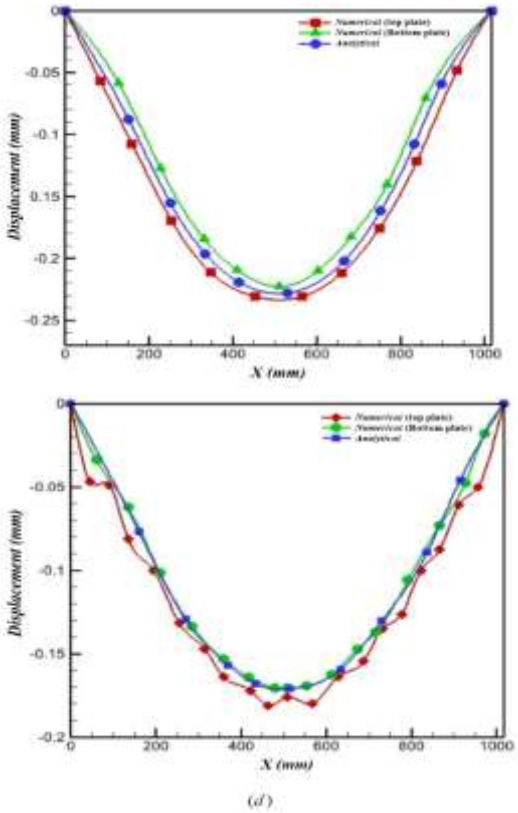

Fig. 11. Comparison of deflection for varying thickness ratios (a) t/l=0.004, (b) t/l=0.006, (c) t/l=0.008, (d)= t/l=0.01

A detailed evaluation of thickness effects also enabled assessment of the validity range of the homogenisation method. For a face-sheet thickness of 4 mm, numerical–analytical discrepancies reached 8.1% (top face) and 19.19% (bottom face), indicating insufficient accuracy of the homogenised CPT model. At 5 mm, the deviations remained elevated due to pronounced local bending and stress gradients.

However, at a thickness of 6 mm, the discrepancy decreased sharply to 1.3% (top face) and 2.6% (bottom face), demonstrating excellent agreement. For a thickness of 8 mm, the errors (6.3% and 1.0%) remained within acceptable limits. At 10 mm, however, the deviations increased again to 17.46% and 10.76%.

This behaviour indicates that the increased discrepancy at a face-sheet thickness of 10 mm does not arise from an inherent limitation of Classical Plate Theory, but from a breakdown of the scale-separation assumption underlying the homogenisation approach. When the bending rigidity of the face sheets becomes much larger than that of the corrugated core, localised face–core interaction effects develop that cannot be captured by the equivalent orthotropic model.

Deformation contours from the finite element model for t = 10 mm (Figure 12) reveal a face-sheet-dominated bending response, with

pronounced local curvature near the face–core interface, indicating loss of deformation uniformity at the corrugation length scale.

Accordingly, the homogenised analytical model remains accurate within:

- t/l = 0.06–0.08
- Face-sheet thickness ≥ 6 mm

Within this range, the bending contributions of the core and face sheets remain comparable, preserving the scale separation required for accurate homogenisation-based CPT predictions.

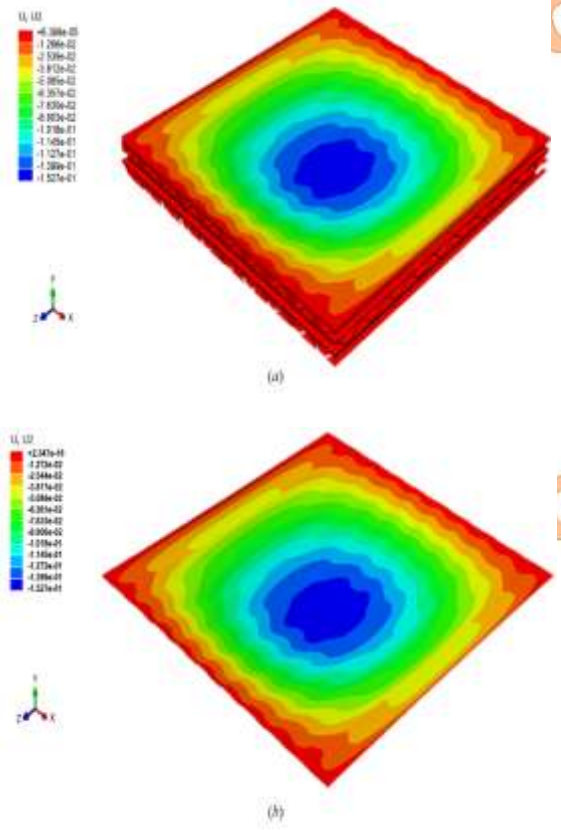

Fig. 12. Contour of deflection for face sheet thickness t=10 mm (a) sandwich panel, (b) top plate.

4.3. Stress Distribution and Critical Regions

The von Mises stress distribution across the sandwich panel exhibits a repeating half-wave pattern along the central region, reflecting the periodic geometry of the orthogonal trapezoidal corrugated core. This region, therefore, served as the primary focus for evaluating the sensitivity of stress behaviour to geometric parameters.

To assess the influence of core geometry, the corrugation height (f) and crown width (a) were systematically varied. As shown in Tables 9 and 10, increasing the core height leads to a substantial reduction in von Mises stress. This decrease is attributed to the enhanced bending stiffness generated by taller corrugation webs, which promote more efficient load transfer through the geometry-induced orthotropic stiffness rather than material anisotropy. In contrast, increasing crown width results in a gradual rise in stress because the number of corrugation cells per unit span decreases, reducing the effective stiffness along the load-bearing direction.

Table 9. Von Mises stress values for different heights (f) with a constant crown value (a)

f (mm)	a (mm)	f/a	σ_{mises} (MPa)
12.7	25.4	0.5	12.3
17.7	25.4	0.7	6.5
22.7	25.4	0.9	5.1

Table 10. Von Mises stress values for different crown values (a) with a constant height (f)

a (mm)	f (mm)	a/f	σ_{mises} (MPa)
25.4	12.7	2	12.3
30	12.7	2.4	13.0
40	12.7	3.1	14.05

The effect of face-sheet thickness (t) is summarised in Table 11. Increasing t markedly decreases stress—up to 45% between 5 mm and 10 mm—due to enhanced local bending resistance of the stiffer outer layers. A similar trend is observed for the corrugated sheet thickness, indicating that both bending and shear stiffness contributions scale directly with thickness for isotropic aluminium.

Table 11. Von Mises stress values for different flat sheet thicknesses

t (mm)	σ_{mises} (MPa)
5	13.2
6	12.3
8	8.5
10	7.3

A comparison between analytical and numerical predictions is given in Table 12. The error remains below 7%, confirming that the homogenisation-based CPT model reliably captures the global stress response within the validated thickness range. The small deviations arise from local bending and shear effects that are not fully represented in Classical Plate Theory but are accurately captured in the detailed 3D finite element model.

Table 12. Comparison of numerical and analytical solutions

t (mm)	Numerical σ_{mises} (MPa)	Analytical σ_{mises} (MPa)	Error (%)
6	12.3	13.13	6.3
7	10.7	11.5	6.95

Representative stress contours for selected cases are shown in Figure 13.

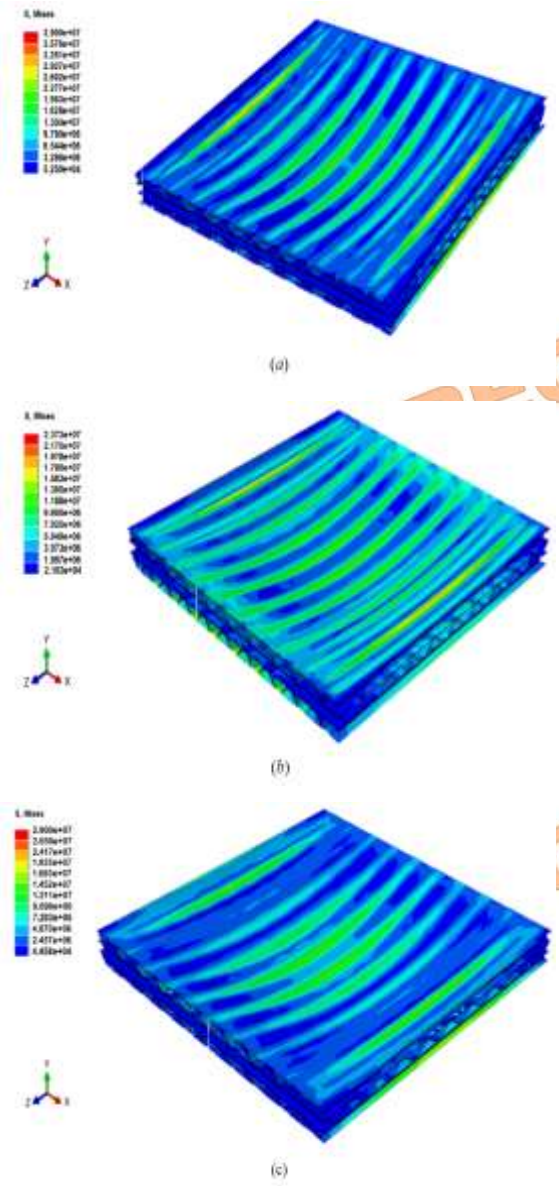

Fig. 13. Contour of von Mises stress distribution for (a) reference geometry, (b) f/a=0.7, (c) t=8 mm

Stress concentrations consistently occur near the core–face-sheet interfaces, especially at crown junctions where sharp geometric transitions induce local bending and slope discontinuities. Increasing face-sheet thickness effectively reduces these peaks by distributing load over a stiffer outer layer. Conversely, excessively large wave heights may introduce abrupt curvature changes along the corrugation profile, which intensify stress concentrations even as global stiffness improves—explaining the observed ~6% stress increase for high f ratios in specific configurations.

Overall, the results confirm that the stress behaviour is dominated by geometry-induced orthotropy, and that the homogenised model remains credible for predicting stress distributions within the established validity range.

4.4. Implications for Design and Application

The combined deflection and stress analyses provide practical guidelines for the design of aluminium sandwich panels with orthogonal trapezoidal corrugated cores. For applications where minimising global deflection is the primary objective—such as lightweight aerospace skins or structural panels subjected to distributed loading—designs should prioritise larger wave heights, moderate crown widths, and increased face-sheet thickness. These parameters significantly enhance bending rigidity through geometry-induced orthotropic stiffness, even though the constituent material remains fully isotropic.

In stress-critical environments, such as marine structures or pressurised compartments, moderate wave heights are preferable to avoid sharp geometric transitions that may introduce localised stress intensification. In all examined configurations, increasing face-sheet thickness proved beneficial, reducing peak von Mises stresses while simultaneously improving overall structural stiffness.

The validated homogenisation-based analytical model serves as an efficient tool for rapid design exploration, greatly reducing the reliance on computationally intensive full 3D finite element simulations. Nevertheless, the model exhibits limitations at extreme geometric ratios—particularly very large wave heights or excessively thick face sheets—where local bending and shear effects exceed the assumptions of Classical Plate Theory. In such cases, targeted FE simulations remain necessary to ensure accuracy.

Future developments should extend the current framework to dynamic, impact, and fatigue loading scenarios, investigate hybrid or graded corrugation patterns, and integrate data-driven optimisation techniques to further enhance performance and expand the applicability of geometry-based homogenisation approaches.

5. Conclusions

This study presented a comprehensive analytical–numerical investigation into the mechanical behaviour of aluminium sandwich panels featuring orthogonal trapezoidal corrugated cores under uniform transverse loading. By integrating a homogenisation procedure based on strain-energy equivalence with Classical Plate Theory (CPT), and validating the resulting analytical predictions through

detailed 3D finite element simulations, a reliable and computationally efficient framework was established for predicting global deflection and stress responses in these geometrically complex structures.

In this context, the present paper systematically consolidates and extends the authors' earlier postgraduate research by formalising the homogenisation–CPT framework, broadening the geometric parametric scope, and translating the outcomes into validated, design-oriented guidelines with direct relevance to lightweight structural applications.

The parametric results demonstrated that the mechanical response is governed primarily by geometric configuration rather than material directionality, as both the core and face sheets were modelled as isotropic aluminium. Increasing the wave height from 10 to 30 mm reduced maximum deflection by approximately 18%, while increasing face-sheet thickness produced up to a 12% reduction in peak von Mises stress. Variations in crown width, half-wave length, and thickness ratios further highlighted the role of corrugation density and face-sheet bending rigidity in enhancing stiffness and mitigating stress concentrations. These findings confirm that geometry-induced orthotropy, rather than material anisotropy, provides the dominant contribution to stiffness tailoring in orthogonal corrugated configurations.

The homogenisation approach proved highly effective within the validated design range, with analytical predictions deviating from finite element results by only about 2% for global deflection and less than 7% for stress. This close agreement confirms that the three-dimensional corrugated architecture can be accurately represented by an equivalent orthotropic plate when geometric ratios fall within realistic engineering bounds. The established validity range—particularly thickness ratios of t/l = 0.06–0.08 and face-sheet thicknesses of ≥ 6 mm—provides practical guidance for confidently applying homogenisation-based analytical tools in early-stage design. At the same time, the observed stress concentrations at core–face-sheet interfaces underscore regions susceptible to failure initiation and indicate where targeted reinforcement may be beneficial.

From a design perspective, the results indicate that taller corrugations and thicker face sheets are advantageous for stiffness-critical applications, whereas moderate wave heights are more suitable for stress-sensitive environments such as marine structures or components subjected to localised loads. Overall, the trends identified here provide actionable guidelines for tailoring geometry to achieve the desired balance between stiffness and strength.

Future work should address remaining limitations, including the effects of dynamic and cyclic loading, material nonlinearity, and potential debonding at adhesive interfaces. Experimental validation is recommended to complement the numerical findings, and further exploration of hybrid or functionally graded corrugated configurations may offer new opportunities for enhancing structural efficiency. Collectively, the outcomes of this research establish a robust foundation for the design, optimisation, and practical implementation of orthogonal corrugated-core sandwich panels in high-performance engineering applications.

Nomenclature

Geometric Parameters

h	Corrugation wave height
w	Crown width of trapezoidal corrugation
f	Corrugation (vertical) height used in parametric studies
a	Crown width (spanwise crown parameter used in parametric studies)
c	Half-wavelength
t_c	Core sheet thickness
t_f	Face-sheet thickness
l	Inclined segment length
L	Developed length within one half-period
$f(x)$	Piecewise function describing the trapezoidal profile
R(x)	Mid-surface position vector

Material/Lamina Properties

E	Young's modulus
ν	Poisson's ratio
ρ	Density
Q_{11}, Q_{12}, Q_{22}, Q_{66}	Reduced stiffness components (material coordinates)

$[\bar{Q}]_k$ Transformed reduced stiffness matrix of the k-th layer

z_k Distance of the k-th layer from the global mid-plane

Displacement Field (CPT)

$u(x, y, z)$ In-plane displacement along x

$v(x, y, z)$ In-plane displacement along y

$w(x, y)$ Transverse displacement

$u_0(x, y)$ Mid-surface displacement along x

$v_0(x, y)$ Mid-surface displacement along y

$w_0(x, y)$ Mid-surface deflection

Strains and Curvatures

$\varepsilon_x^{\,0}, \varepsilon_y^{\,0}$ Membrane strains

$\gamma_{xy}^{\,0}$ Shear strain

κ_x, κ_y Bending curvatures

κ_{xy} Twisting curvature

Laminate Stiffness Components

[A] Extensional stiffness matrix

[B] Coupling stiffness matrix

[D] Bending stiffness matrix

A_{ij} Extensional stiffness components

B_{ij} Coupling stiffness components

D_{ij} Bending stiffness components

Generalized Forces & Moments

N_x, N_y, N_{xy} In-plane membrane forces

M_x, M_y, M_{xy} Bending and twisting moments

Loads & Stress Measures

q Transverse uniform load

σ_x, σ_y Normal stresses

τ_{xy} Shear stress

W_{mn} Fourier/Navier coefficient of deflection

Numerical Modelling Symbol

S_{max} Maximum von Mises stress

w_{max} Maximum transverse deflection

Statistical Validation Metrics

$RMSE$ Root Mean Square Error

R^2 Coefficient of determination

Coordinates

x, y In-plane coordinates

z Through-thickness coordinate

Funding Statement

This work was supported by the University of Sistan and Baluchestan under a student research grant.

Conflicts of Interest

The authors declare no competing interests.

References

[1] Sutherland, L. S., et al. (2012). Dynamic and quasi-static testing of glass fiber reinforced polymer composites for marine applications. *Composites Part B: Engineering*, 43(7), pp. 3233–3248. https://doi.org/10.1016/j.compositesb.2012.03.053.

[2] Ivazian, A., et al. (2021). Reinforcement of sandwich panels using resin pins: Improvement in flexural and indentation behaviour. *Composite Structures*, 267, 113879. https://doi.org/10.1016/j.compstruct.2021.113879.

[3] Li, Y., et al. (2020). Modelling and analysis of sandwich panels with corrugated cores. *Composite Structures*, 238, 111938. https://doi.org/10.1016/j.compstruct.2020.111938.

[4] Abada, D. R., & Ibrahim, A. (2023). Blast response of sandwich panels with triangular and trapezoidal corrugated cores. *Composite*

Structures, 301, 116145. https://doi.org/10.1016/j.compstruct.2022.116145.

[5] Radojković, M., Stojanović, B., Milojević, S., Marić, D., Savić, S., Skulić, A., & Krstić, B. (2023). Square openings are sources of stress concentration in parts of machines and devices. *Tehnički vjesnik*, 30(2), pp. 474-480. https://doi.org/10.17559/TV-20221215144619.

[6] Stojanović, B., & Milojević, S. (2017). Characterization, manufacturing and application of metal matrix composites. In M. C. Wythers (Ed.), *Advances in materials science research* (Vol. 30, pp. 83–113). Nova Science Publishers.

[7] Jin, F., et al. (2023). Dynamic response of sandwich panels with auxetic honeycomb core under blast loading. *Composite Structures*, 305, 116651. https://doi.org/10.1016/j.compstruct.2022.116651.

[8] Mahdiabadi, M. K., Ghasemi, S. H., & Mohammadi, H. (2024). Numerical and experimental study on energy absorption capability of advanced corrugated sandwich panels. *Thin-Walled Structures*, 194, 110779. https://doi.org/10.1016/j.tws.2023.110779.

[9] Long, C., et al. (2018). Numerical modeling of failure modes in foam sandwich laminate panels. *Composites Part B: Engineering*, 146, pp. 127–136. https://doi.org/10.1016/j.compositesb.2018.03.037.

[10] Xia, F., Durandet, Y., Tan, P. J., & Ruan, D. (2022). Parametric study on the load-bearing capacity of corrugated-core sandwich beams under combined loading. *Composite Structures*, 280, 114910. https://doi.org/10.1016/j.compstruct.2021.114910.

[11] Matsunaga, H. (2008). A higher-order deformation theory for composite sandwich plates subjected to various loadings. *Composite Structures*, 82(4), pp. 499–512. https://doi.org/10.1016/j.compstruct.2007.02.011.

[12] Zhen, X., & Ren, W. (2019). Transverse normal strain in simply supported sandwich plates: An improved analytical solution. *International Journal of Mechanical Sciences*, 163, 105092. https://doi.org/10.1016/j.ijmecsci.2019.105092.

[13] Huang, L., Yuan, H., & Zhao, H. (2023). An FEM-based homogenization method for orthogonal lattice metamaterials within micropolar elasticity. *International Journal of Mechanical Sciences,* 238, 107836. https://doi.org/10.1016/j.ijmecsci.2022.107836.

[14] Hashemi-Karouei, S. H., Moazemi Goudarzi, A., Morshedsolouk, F., & Mousavi Ajarostaghi, S. S. (2020). Analytical and finite element investigations of the cross-arranged trapezoidal- and sinusoidal-corrugated-cores panels. *Mechanics of Advanced Materials and Structures*, 27(19), pp. 1626–1636. https://doi.org/10.1080/15376494.2020.1834652.

[15] Kamareh, F., Soleimanimehr, H., Mosalman, Y., & Mirtalaei, S. M. (2024). Two-scale modeling and analysis of sandwich beams with functionally graded face sheets and corrugated cores. *International Journal of Mechanical Sciences*, 265, 108278. https://doi.org/10.1016/j.ijmecsci.2023.108278.

[16] Wang, Y., Wang, K., & Zhang, C. (2024). Applications of artificial intelligence/machine learning to high-performance composites. *Composites Part B: Engineering*, 285, 111740. https://doi.org/10.1016/j.compositesb.2024.111740.

[17] Briassoulis, D. (1986). Equivalent orthotropic properties of corrugated sheets. *Computers & Structures*, 23(2), pp. 129–138. https://doi.org/10.1016/0045-7949(86)90184-0.

[18] Reddy, J. N. (2004). Mechanics of Laminated Composite Plates and Shells: *Theory and Analysis*. 2nd ed., CRC Press, Boca Raton, FL.